Optical and Quantum Electronics **11** (1979) 265–273

Variation of pulse delay with stress and temperature in jacketed and unjacketed optical fibres

A. H. HARTOG, A. J. CONDUIT, D. N. PAYNE
Department of Electronics, University of Southampton, Southampton, UK

Received 7 December 1978

The stability of optical-fibre delay lines is assessed by means of measurements of pulse transit times in unjacketed silica-based fibres. Data obtained for the effect of longitudinal stress and temperature are used to interpret the time delays found in jacketed fibres. It is shown that the application of close-fitting plastic cabling materials results in a residual fibre stress which is both temperature and humidity dependent.

1. Introduction

Measurements of the pulse transit time in an optical fibre can be used to reveal several interesting properties relevant to the transmission medium. For example, the wavelength dependence of pulse delay has been used to determine the material dispersion parameter in multimode fibres [1, 2] and the chromatic dispersion in single-mode fibres [3]. Moreover, the inherent stability of the delay and the high bandwidth attainable has led to the employment of optical fibres as delay lines in signal processing applications [4]. Delay–bandwidth products of greater than 5000 are possible. The high delay stability has also suggested the use of fibres as strain gauges [5] and for synchronizing of remote events in high energy physics.

With a dual objective, we have performed and report in this paper further measurements of pulse transit time in optical fibres. Firstly, the stability of the time delay has been evaluated for variations in temperature and axially-applied stress in order to provide data for the design of optical delay lines. Both unjacketed and plastic-clad fibres have been tested and it is shown that the application of a secondary nylon coating considerably degrades the delay stability.

A second objective results from the observation that the pulse delay is dependent on fibre tension, suggesting the use of the measurement as a diagnostic test for residual stress levels in optical cables. The latter measurement is of some importance to cable designers, since ideally the fibre should be neutrally stressed in order to avoid static fatigue and microbending effects. Refinements to our previously reported delay-measurement technique [2] have resulted in improved long-term stability and this has permitted experiments to be undertaken to determine the residual compressive stress level in the fibre following the application of a nylon over-jacket. In addition, the effect of water ingress on the cable has been assessed.

2. Theory

The pulse transit time τ in a fibre of length L may be found approximately from

$$\tau = \frac{L}{c} N_1 \qquad (1)$$

where c is the speed of light *in vacuo* and

$$N_1 = n_1 - \lambda \frac{dn_1}{d\lambda}$$

is the material group index. Here n_1 is the refractive index at core centre and λ the wavelength. Longitudinally-applied stress σ and temperature T produce changes in both fibre length and refractive index, each of which affect the transit time. The variation of pulse delay with temperature is given by

$$\frac{d\tau}{dT} = \frac{1}{c}\left(N_1\frac{dL}{dT} + L\frac{dN_1}{dT}\right) \quad (2)$$

and the variation with stress by

$$\frac{d\tau}{d\sigma} = \frac{1}{c}\left(N_1\frac{dL}{d\sigma} + L\frac{dN_1}{d\sigma}\right) . \quad (3)$$

Values for the thermal expansion coefficient dL/dT and the temperature coefficient of refractive index dn_1/dT ($\simeq dN_1/dT$) are given in [6] for bulk fused silica. The respective contributions of the two terms to the total variation of pulse delay are shown in Table I. It may be seen that the two effects are the same in sense and that the refractive index variation dominates. Summing the two effects leads to a combined change with temperature of 40 ps $km^{-1} K^{-1}$.

The change in refractive index with applied stress is a result of the stress–optical effect. For a purely axial stress, photo-elastic theory gives

$$\frac{dN_1}{d\sigma} \simeq \frac{dn_1}{d\sigma} = \frac{1}{3}(A + 2B) \quad (4)$$

where A is the isostatic pressure dependence of index [7] and B is the stress-induced birefringence [8]. In addition, fibre tension produces an elongation which may be found from Young's modulus $E = Ld\sigma/dL$. Table I gives the time-delay components resulting from the known values of $dn_1/d\sigma$ and $dL/d\sigma$ for silica [7, 8] and reveals that the two terms contribute an effect of similar magnitude, but of opposite sense, to the overall variation of time delay with applied axial stress. In contrast to the dependence on temperature, it is now the change in fibre length which dominates the change in index, giving an overall effect of 47.1 ps km^{-1} for a stress of 1 MPa.

Departures from the above calculated values are expected in practice due to the presence of graded concentrations of P_2O_5 and GeO_2 in the fibre cores, and the chilled state of the fibres. The latter is a result of the rapid cooling experienced during the fibre drawing process.

The application of a close-fitting polymer over-jacket to the fibre modifies the temperature dependence of pulse delay, owing to the large expansion coefficient of plastic materials. Using a simplified elastic model of fibre and coating, we arrive at the following expression for the effect of temperature on a jacketed fibre:

$$\frac{d\tau}{dT_{\text{jacketed}}} = \frac{A_P}{A_F}E_P k_P\left(\frac{d\tau}{d\sigma}\right)_F + \left(\frac{d\tau}{dT}\right)_F \quad (5)$$

where A is the cross-sectional area, E the Young's modulus and k the expansion coefficient. The subscripts P and F refer respectively to the plastic over-jacket and the fibre. For a typical fibre of 125 μm diameter having a primary silicone coating of 250 μm diameter and a 500 μm diameter nylon over-jacket, for which $E_P = 3.1 \times 10^9$ Pa, $k_p = 8.3 \times 10^{-5} K^{-1}$, we find the variation of pulse delay with temperature to be 185 ps $km^{-1} K^{-1}$ (neglecting the contribution of the soft silicone buffer layer). The delay stability is thus expected to be nearly an order of magnitude worse than for an unjacketed fibre.

3. Experimental procedure

An optical pulse of 0.35 ns duration from a GaAs injection laser operating at 0.9 μm is launched into the fibre and the pulse transit time measured using a time-delay generator and sampling oscilloscope. In order to improve the timing stability and eliminate errors which may result from long-term

TABLE I Calculated components of the temperature and stress dependence of time delay in bulk fused silica. The bracketed figures refer to the experimentally-determined values for unjacketed silica fibres doped with P_2O_5/GeO_2

Component	With temperature (ps $km^{-1} K^{-1}$)	With stress (ps km^{-1} MPa)
effect on delay due to variation of index N_1	38	−21.6 (−16.9)
effect on delay due to variation of length L	2	68.7 (70.6)
combined calculated effect on delay	40 (35.7)	47.1 (53.7)

variations in the laser turn-on time, a technique has been evolved which uses a marker pulse reflected from the input to the test fibre to provide a time reference. As shown in Fig. 1, the laser output is focused into a 25 m 'pigtail' of graded-index fibre, to which the test fibre is butt-coupled. The 8% Fresnel reflection which occurs at the joint returns a pulse to the fibre input, from where it is directed to a silicon avalanche photodetector by means of a 50% beam splitter. An aluminium mirror butted against the far end of the test fibre similarly returns a pulse to the APD. The time difference between the two pulses is found by positioning each to the same point on a sampling oscilloscope display using a variable pulse-delay generator. The electrical delay introduced in each case is then accurately determined with a time interval counter. The difference between the readings obtained for the reference pulse and the pulse returned from the remote end of the test fibre gives double the fibre transit time.

The advantage of the above technique is that long-term trigger-delay drifts in the timing circuitry can be eliminated, since they are common to both measurements. Furthermore, the back-reflection technique improves the sensitivity of the experiment, since it doubles the effective length of the fibre. Two further considerable advantages for field measurements are that access to only one end of the fibre is required and that test fibres may be easily interchanged without the necessity for re-alignment of the optics.

Pulse-delay measurements were performed on fibres having only a primary coating of silicone rubber and on fibres jacketed with a secondary coating of nylon. The former were made to assess the intrinsic effects of tension and temperature on silica-based fibres (the silicone rubber contributes little to the observed delays) and to compare the results with those calculated previously. The measurements on nylon-jacketed fibres could then be interpreted in the light of the known behaviour of the fibre under stress.

The variation of pulse delay with applied tension in unjacketed fibres was evaluated by horizontally suspending the fibre between two sheaves of eight low-friction pulleys spaced up to 90 m apart. Intermediate supports were provided for the fibre strands at intervals of approximately 20 m so as to reduce sag. A calibrated tension could be evenly distributed amongst the fibre sections by applying a known force to one of the pulley blocks and the resulting elongation determined by noting the block displacement. Measurements were made on three graded-index fibres having similar $GeO_2/P_2O_5/SiO_2$ core compositions in effective lengths (2 x actual length) ranging from 0.67–1.6 km.

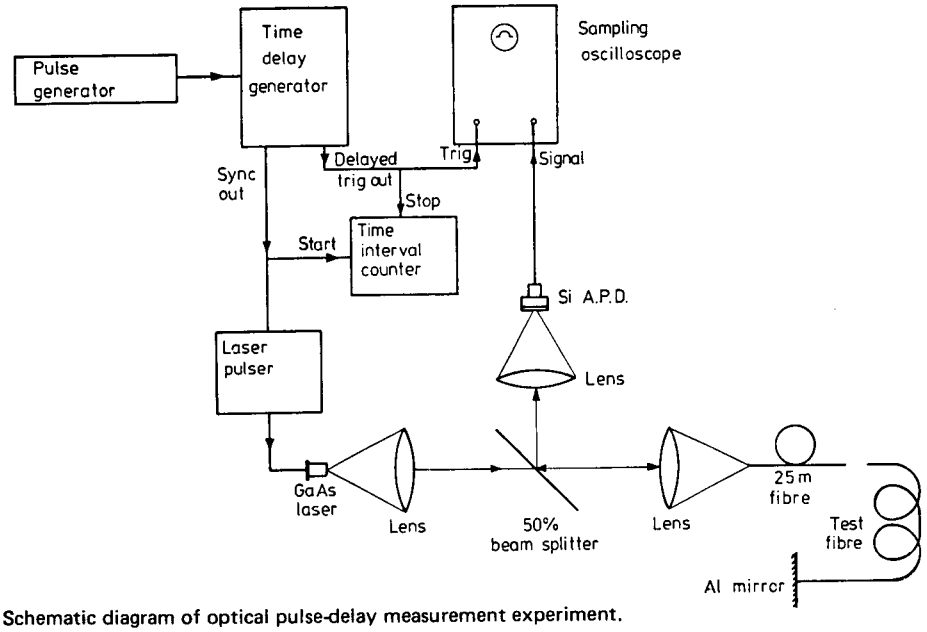

Figure 1 Schematic diagram of optical pulse-delay measurement experiment.

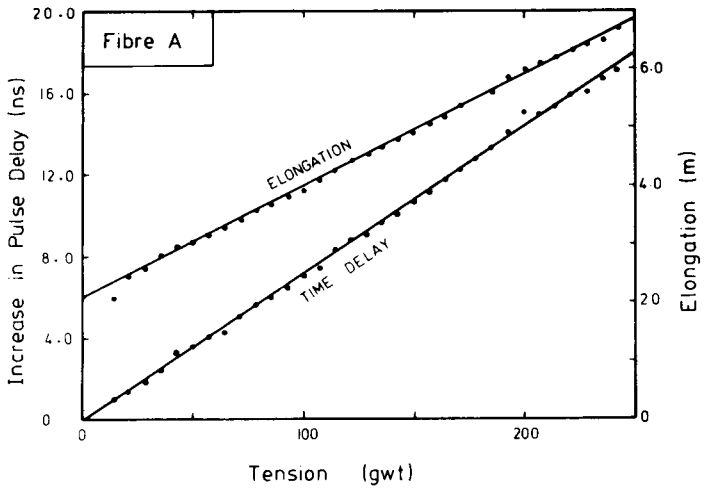

Figure 2 Variation of pulse-delay and fibre extension with applied tension for Fibre A (Table II). The fibre is unjacketed and has an effective length of 1.6 km.

The temperature-dependence of delay was assessed in both unjacketed and jacketed fibres by removing them from the drum and freely suspending the coils in a chamber whose temperature could be controlled over the range − 30 to + 100° C to within ± 0.5° C. Care was taken to ensure that no additional stresses were applied to the fibre. The effect of water and salt water on the jacketed fibres over the temperature range 0–50° C was determined by immersing the freely coiled fibres in a temperature-controlled liquid bath. The fibres were conditioned to their environments (air or liquid) by performing a stabilizing soak at elevated temperature for periods of up to a few days.

4. Experimental results

4.1. Effect of applied tension on unjacketed fibres

Transit time measurements were made on an unjacketed, silicone-coated fibre, Fibre A, with characteristics given in Table II. The experimental results for the variation of both pulse delay and fibre elongation with tension are shown in Fig. 2.

The extension curve exhibits a zero offset which is attributed to the uptake of the sag in the fibre at low values of tension; the absence of such an effect in the time-delay curve indicates that the measured tension accurately reflects that applied to the fibre.

A straight line least-squares fit to the data of Fig. 2 reveals a value of 53.7 ps $km^{-1} MPa^{-1}$ for the variation of time delay with applied tensile stress. This is substantially larger than the calculated figure of 47.1 ps $km^{-1} MPa^{-1}$ for fused silica given in Table I, even taking into account the uncertainty in the experimental value of 3%, resulting mainly from the error in the fibre diameter measurement. On the other hand, the least-squares fit to the extension data indicates that the contribution of the change in length to the variation in time delay is 70.6 ps $km^{-1} MPa^{-1}$, which is in close agreement with the value of 68.7 ps $km^{-1} MPa^{-1}$ calculated from the tabulated results

TABLE II Properties of fibres used in pulse-delay measurements. All fibres have $P_2O_5/GeO_2/SiO_2$ cores and a B_2O_3/SiO_2 buffer layer

Property	Fibre A	Fibre B	Fibre C
approximate length, m	800	600	600
numerical aperture	0.21	0.21	0.21
core diameter, μm	65	65	65
fibre diameter, μm	122.5	122.5	125
silicone coating diameter, μm	250	250	250
nylon diameter, μm	unjacketed	unjacketed	500

for pure silica [7]. Thus the major departure from the fused silica values lies in the effect of stress on the glass refractive index, where a shortfall of some 20% is found (Table I). This is perhaps not surprising in view of the presence of P_2O_5 and GeO_2 in the fibre core and the large differences found in practice between the stress–optical coefficients of glasses having different compositions. Measurements on two other fibres having GeO_2/P_2O_5-doped cores produced similar results, indicating that the discrepancy could be attributed to a material property.

4.2. Effect of temperature on unjacketed fibres

Pulse delays were measured as a function of temperature in a 600 m length of silicone-coated fibre, Fibre B, (Table II) produced from the same preform as Fibre A. The results over the temperature range − 30 to + 100° C are shown in Fig. 3, normalized to a fibre length of 1 km. The actual experimental length was determined by measuring the time delay at 20° C and comparing this with the delay measured in an accurately known short length of fibre. The latter gave a value for the group index of 1.4798 ± 0.04%.

The least-squares fit to the data of Fig. 3 gives a delay variation of 35.7 ps $km^{-1} K^{-1}$, a value which is somewhat smaller than the calculated figure of 40 ps $km^{-1} K^{-1}$ for pure silica. The experiment repeated in the reverse temperature direction produced a similar result and showed no hysteresis in the measurement.

4.3. Residual fibre stress introduced by jacketing with nylon

During the cabling process, stresses are unavoidably applied to the optical fibre and some of these may remain in the finished product. For example, the high-temperature extrusion of the secondary coating is expected to result in longitudinal compression of the fibre on cooling, owing to the difference in expansion coefficients between glass and plastic. Although compressive stresses applied to the fibre may possibly result in improved strength characteristics, they may also have detrimental effects such as increased microbending losses.

An experiment was conducted on 600 m of fibre, Fibre C, (Table II) from the same production batch as those used previously, in order to determine the residual stesses within the fibre and thus demonstrate the use of pulse-delay measurements for cable diagnostics. Initially, the silicone-coated fibre was freely suspended in a stress-free state and the pulse transit time determined. A secondary layer of nylon was then applied by extrusion to give an outer diameter of 0.5 mm. Care was taken to ensure that all fibre pieces broken off during the extrusion process and for the purposes of end preparation were taken into account.

It was found that the transit time after jacketing had decreased by 2.44 ns km^{-1} which from the stress/pulse delay calibration previously performed (Section 4.1) indicates a residual compressive stress of 45 MPa (a compressive force

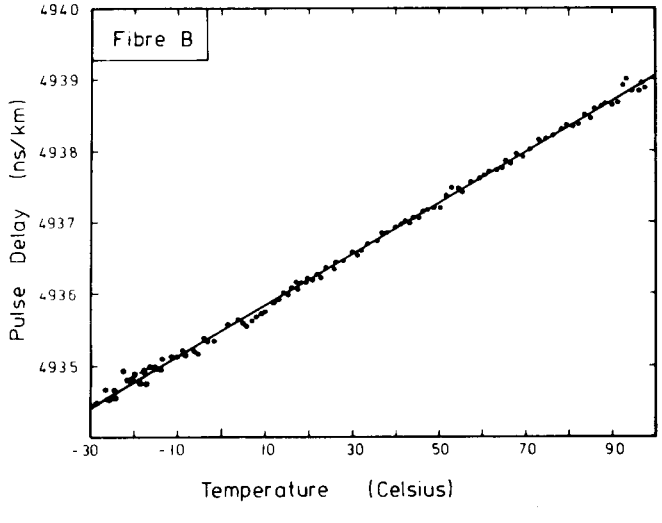

Figure 3 Pulse-delay normalized to a length of 1 km as a function of temperature for an unjacketed fibre, Fibre B (Table II).

of 58 g-wt). Such a figure is an order of magnitude less than that estimated from the known [9] expansion coefficient and Young's modulus of nylon, although it should be noted that an exact analysis is complicated by the fact that the remaining stress is dependent on the extrudate cooling conditions and the time allowed for stress relief by plastic creep. The relatively low level of residual compression found in the fibre indicates that considerable stress relief had taken place in the period immediately following extrusion.

4.4. Delay stability in jacketed fibres

The temperature stability of pulse delay was investigated in Fibre C, after jacketing with nylon as described above. After an initial annealing period during which the transit time decreased slightly, the fibre was freely suspended in air and the time delay monitored as the temperature was cycled over the range − 30 to + 50° C. Several interesting effects were observed which could be attributed to the known creep behaviour of plastic materials. The thermal history of the fibre/plastic composite and the duration of the experiment were found to influence the time delay measured at any point in the temperature range. For example, static measurements at − 30° C following a prolonged period spent at 50° C would result in an upward drift in pulse delay of as much as 4 ns km^{-1}. Conversely, measurements at 50° C after stabilization at − 30° C produced a downward drift of similar magnitude. Furthermore, the delay was observed to exhibit hysteresis.

This behaviour is illustrated in Fig. 4. The curves show an experiment in which the temperature was continuously cycled at a rate of approximately 10° C/hour. One and three-quarter cycles were performed under these conditions (solid lines, curves 1–4) and are seen to produce almost coincident time-delay hysteresis loops. Curve 5 (dashed), on the other hand, shows a measurement taken in the direction of increasing temperature after the above temperature cycles had been interrupted at − 30° C for 12 hours. The static period has resulted in an upward drift in pulse delay of 1 ns, which, on resumption of temperature cycling, leads to a curve lying above those previously determined, although tending towards them at higher temperatures. Similarly, curve 6 (dashed) shows the effect of a 12 hour pause at 50° C, which produced a 0.5 ns drop in delay. The difference is gradually eliminated as the temperature is cycled.

The departure of the delay curves in Fig. 4 from the simple straight-line characteristic exhibited by the unjacketed fibre (Fig. 3) is the result of the mechanical properties of the secondary coating and the forces it exerts on the fibre. Plastics by their very nature do not exhibit simple elastic and thermal behaviour [10–12]; unlike silica, they are non-Hookean and such quantities as Young's modulus and thermal expansion coefficient are dependent on the magnitude of the applied load, the time scale and the temperature of the experiment. Furthermore, the thermal history, water content and degree of crystallinity of the plastic affect their properties.

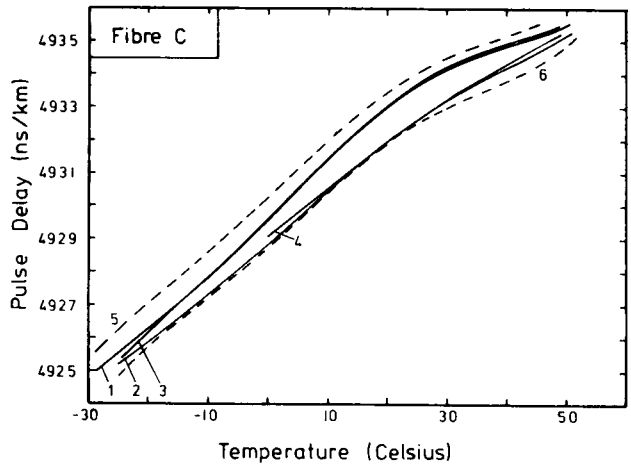

Figure 4 Variation of pulse-delay with temperature for Fibre C, having a nylon jacket. The delay is normalized to a fibre length of 1 km. Solid lines are for continuous temperature cycling, dashed lines show effect of pausing at − 30° C and 50° C.

Clearly, the hysteresis and time-dependent behaviour of the pulse delay shown in Fig. 4 are a result of stress relief in the fibre caused by plastic creep of the nylon over-jacket. The reason, however, for the marked change in slope at approximately 30° C is not at present understood, although we note that both the expansion coefficient and tensile modulus of nylon vary non-linearly with temperature. As a consequence of the effect, the temperature coefficient of time delay is no longer uniquely defined, being both time and temperature dependent. However, averaging the slopes of curves 1 and 2 below 10° C leads to a working figure of 170 ps $km^{-1}K^{-1}$. This is in good agreement with the value of 185 ps $km^{-1}K^{-1}$ calculated previously.

The temperature stability of time delay in the jacketed fibre, Fibre C, should be compared with that of the primary-coated fibre, Fibre B, for which a value of 35.7 ps $km^{-1}K^{-1}$ was found. The application of the protective jacket degrades the stability by nearly a factor of five. Furthermore, it should be recognised that the incorporation of the jacketed fibre into a larger cable structure having the same high expansion coefficient will produce a still greater variation.

4.5. Effect of water ingress on jacketed fibres

The influence of moisture ingress on the performance of jacketed fibres was assessed by immersing Fibre C loosely coiled in a water bath. Experiments were also conducted whilst immersed in a 20 wt% aqueous NaCl solution. Sufficient time was allowed for the fibre to reach equilibrium (72 hours and 36 hours at 50° C for water and NaCl solutions, respectively [9]). The pulse-delay performance for temperature cycles over the range 0–50° C is given in Fig. 5. Also shown are the results previously presented (Fig. 4) for the same fibre, Fibre C, suspended in air and, to aid comparison, for the unjacketed fibre, Fibre B (Fig. 3). The results are all normalized to a length of 1 km. This was achieved as outlined in Section 4.2 by precisely determining the time delay in the unjacketed fibres and comparison with the delay in a known short length of the same fibre. The length of Fibre C was known from the results obtained prior to extrusion of the plastic jacket. However, confirmation of the measurement was obtained by removal of the jacket in concentrated nitric acid on completion of the temperature experiments. This also served to verify the effect found in Section 4.3, namely that the time delay decreased after jacketing. It was ascertained that removal of the jacket now produced an increase in pulse delay and that the final value was in close agreement with that found prior to extrusion of the nylon.

The curves of Fig. 5 show that both water and salt solutions produce a marked increase in time delay, suggesting that a release of residual compressive fibre stress has occurred. Hysteresis behaviour is observed and curve gradients are closer to that of the unjacketed fibre, indicating that the liquids have caused a softening of the

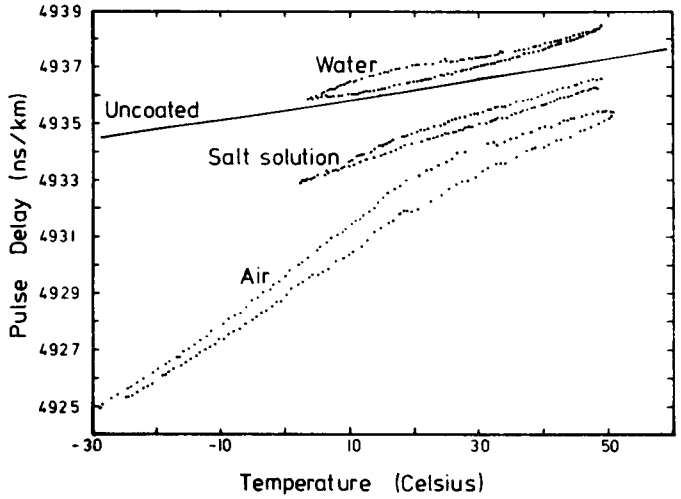

Figure 5 Measured values of pulse-delay versus temperature for a nylon-jacketed fibre, Fibre C (Table II), under various environmental conditions (dots). The solid curve gives time delay for unjacketed fibre, Fibre B (Table II). All curves are normalized to 1 km.

jacketing plastic, i.e. reduced its modulus. In addition, the curve for water immersion lies above that of the unjacketed fibre, indicating that the fibre is in fact in tension. This may be seen more clearly by noting that at any temperature the time-delay difference between the jacketed fibre and the unjacketed one is an indication of the stress that the sheath is applying to the fibre. With the aid of the calibration figure for the dependence of time delay with stress for these fibres, we may map Fig. 5 into the residual stress versus temperature curves shown in Fig. 6, where the negative sign indicates fibre compression.

Fig. 6 reveals that at room temperature the residual compressive longitudinal force exerted on the fibre by dry nylon (after conditioning) is in the region of 100 g-wt. The ingress of water into the plastic has relieved the initial compression which existed after extrusion and in fact has caused the fibre to become tensioned. This effect is consistent with the known [9] volume expansion and reduction of Young's modulus which accompanies water saturation (9.5 wt%) of nylon.

The subsequent immersion in a salt solution caused the fibre to return to compression, although not to the level observed in air. This was accompanied by a significant increase in attenuation (6 dB km^{-1}) with little change in pulse dispersion, an effect which was not observed in water. Furthermore, on removal from the salt solution and drying, the attenuation became so high as to render further measurements impossible. This was found even if the fibre was rinsed in de-ionized water for two days prior to drying; however, re-immersion in water restored the transmission. Similar behaviour was found in aqueous $CaCl_2$ solutions. Clearly the effect is attributable to an increase in microbending loss in the fibre caused by a change in the nylon characteristics. The mechanism whereby such kinking can occur as a result of increased radial pressure exerted by the plastic, but with little change in stress in the axial direction is not at present clear.

Although the levels of salt concentration used in these experiments are high, the effects observed are indicative of the performance of nylon as a jacketing material in hostile environments. A more appropriate choice in these cases would be polypropylene, which exhibits a low level of hygroscopy and high resistance to chemical attack.

Experiments performed on nylon-jacketed fibres immersed in organic solvents such as formaldehyde and glycol–methanol (1 : 1) similarly produced changes in the fibre stress levels, although their effect on pulse dispersion and attenuation have not been measured.

5. Conclusions

Measurements of the stability of the optical pulse delay in both unjacketed and jacketed fibres have been presented. In the case of unsheathed fibres, an evaluation of the dependence of delay on fibre tensile stress and temperature reveals that the

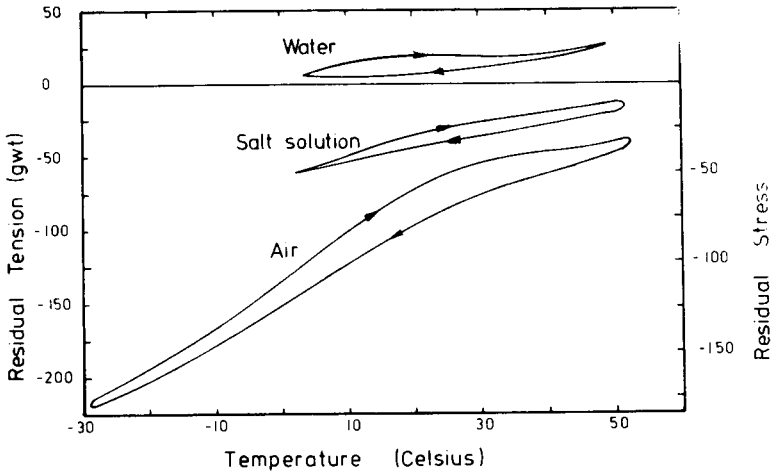

Figure 6 Stress and force exerted on Fibre C by the nylon jacket for various environmental conditions.

effects are linear, having values of 53.7 ps km^{-1} MPa^{-1} and 35.7 ps km^{-1} K^{-1}, respectively. Calculation of the expected values for bulk fused silica indicates that the variation with stress is dominated by the physical change in fibre length and that with temperature by the change in refractive index. Comparison of the silica values with those determined experimentally demonstrates significant departures for P_2O_5/GeO_2-doped fibres, particularly for the stress-induced index change.

For fibres jacketed with nylon, it was observed that the presence of the sheath produced much larger and non-linear excursions of time delay with temperature. The departure of the performance of the jacketed fibre from that of the unclad fibre was used to evaluate the effect of the sheath on residual fibre stress levels. The physical properties of the plastic jacketing material were shown to induce time-delay drift and hysteresis following temperature variations. In addition, the ingress of water modifies the plastic properties and causes significant delay variations. Furthermore, immersion in salt and $CaCl_2$ solutions irreversibly impairs optical transmission, indicating that nylon is unsuitable for use as a cladding material in hostile environments.

From the above we see that the temperature stability of the transit time can be severely degraded by encapsulation of the fibre in plastic materials having a high expansion coefficient. This is a consequence of the sensitivity of the delay to applied longitudinal stress. Thus plastic-jacketed fibres or epoxy-potted coils should not be used in applications which require high time stability, for example in fibre delay lines and strain gauges.

On the other hand, the stress dependence of delay can be used to provide a powerful diagnostic tool for cable stress analysis. This was demonstrated by an experiment to determine the fibre compression induced by application of a nylon jacket, where a residual compressive force of 58 g-wt was found. Application of the method to determine residual stresses after each stage of cable manufacture is possible; for example, after stranding, sheathing and armouring. In addition, it is envisaged that periodic tests on installed cables could be used to provide information on long-term cable creep effects.

Acknowledgements

The authors are grateful to S. R. Norman for fabricating the fibres used in the experiments. Thanks are due to Professor W. A. Gambling for his help and guidance and to members of the Optical Communications Group for useful discussions. Acknowledgements are made to the Association of Commonwealth Universities (A.J.C.) and to the University of Southampton (A.H.H.) and the Pirelli Cable Company (D.N.P.) for financial support.

References

1. B. LUTHER-DAVIES, D. N. PAYNE and W. A. GAMBLING, *Opt. Commun.* **13** (1975) 84–88.
2. D. N. PAYNE and A. H. HARTOG, *Elect. Lett.* **13** (1977) 627–29.
3. K. DAIKOKU and A. SUGIMURA, *ibid* **14** (1978) 149–51.
4. C. T. CHANG, J. A. CASSABOOM and H. F. TAYLOR, *ibid* **13** (1977) 678–80.
5. M. JOHNSON and R. ULRICH, *ibid* **14** (1978) 432–33.
6. 'American Institute of Physics Handbook' (McGraw-Hill, New York, 1972), pp. 4–138.
7. R. BRUCKNER, *J. Non-Crystl. Solids* **5** (1970) 123–75.
8. W. PRIMAK and D. POST, *J. Appl. Phys.* **30** (1959) 781.
9. S. GROSS (Editor) 'Modern Plastics Encyclopedia', (McGraw-Hill, New York, 1969).
10. L. E. NIELSEN, 'Mechanical properties of polymers', (Reinhold Publishing Co., New York, 1962).
11. R. M. OGORKIEWICZ, 'Engineering properties of thermoplastics', (J. Wiley and Sons Ltd., New York, 1970).
12. N. G. MCCRUM, B. E. READ and G. WILLIAMS, 'Anelastic and dielectric effects in polymeric solids', (J. Wiley and Sons Ltd., New York, 1967).

Short Communication

Application of OTDR for thickness monitoring of optical thin films

The optical time-domain reflectometer (OTDR) is normally used to locate breaks and to measure the propagation and splicing losses in fibres and fibre cables [1, 2]. In this communication we report a novel and practical extension of OTDR to thin film deposition technology.

A special interest in the use of interference filters in connection with multimode optical fibres has arisen recently [3, 4]. Here we shall report the fabrication of antireflection coatings and interference filters directly on the end of a multimode fibre by monitoring the film growth during vacuum evaporation with OTDR.

The basic idea in our backscattering arrangement is the same as reported earlier [1, 2] and the extended experimental set-up of our work is seen in Fig. 1. The pulse width of the semiconductor laser SG 2001 was 150 ns. As a photodetector, the avalanche photodiode BPW 28 was used. The sampling oscilloscope (Tektronix 7603 with plug-ins: 7S11, 7S12, S-2 and S-4) was operated in a manual sweep mode, and the horizontal deflection of the cathode ray was placed at the top value of the back-end reflection. The vertical signal of the cathode ray is in turn coupled to a recorder, so that during film deposition we obtain a curve that follows the reflectance change of the fibre end.

The vacuum feedthrough for the optical fibre was accomplished by the aid of a small injection needle filled with vacuum grease (Wacker Hochvakuumfett). Before installing the fibre, the primary coating is first removed from part of the fibre. Because in the evaporation unit there is a separate top plate (see Fig. 1) the end preparation of the fibre can be done only after pushing the fibre through the feedthrough. After the evaporation the fibre can again be withdrawn without damaging the end surface. This makes it possible to use fibres of arbitrary length, and a minimum length of about only 50 m is required for the OTDR.

As a demonstration, the recorder chart curve obtained during CeF_3 ($n_f = 1.63$) evaporation on the graded-index fibre of core diameter 50 μm is shown in Fig. 2. After the evaporation rate has gradually increased to a constant value within the first five minutes, the reflectance of the fibre end varies almost sinusoidally. The reflectance maxima occur at optical thicknesses

$$n_f d = m\lambda/4 \quad (m = 1, 3, 5 \ldots).$$

The typical vacuum pressure was under 10^{-3} Pa.

In Fig. 3 one can see the transmission curve of $\lambda/4$ stack $(HL)^3H$ fabricated by this method using the fibre as a thickness monitor. Here H means a $\lambda/4$-film of ZnS ($n_f = 2.38$) and L is a $\lambda/4$-film of MgF_2 ($n_f = 1.38$). The maximum reflectance of the stack is 95%. This can be compared to the 90% reflectance of aluminium mirrors.

To conclude, we have extended the applicability of the OTDR method to optical thin film deposition. The fibres can be used as a thickness monitor during the evaporation or as a substrate to deposit the fibre end itself. In particular, we have shown that fibres can be inserted into

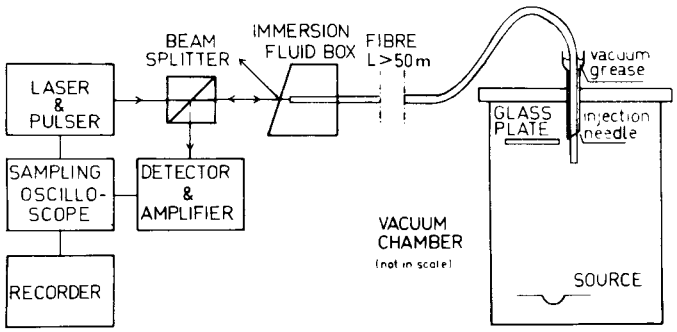

Figure 1 **The experimental arrangement of OTDR applied to thin film monitoring.**